DOI: 10.6060/mhc267110a

A Novel Unsymmetrically Substituted Dibromo-BODIPY Photosensitizer: Synthesis, Photophysical/Photochemical Characteristics and Antimicrobial Activity

Lubov A. Antina,[a] Daria A. Fedorova,[a,b] Artem S. Sherudillo,[a@] Olga V. Miloshevskaya,[a,b] Alexey N. Sivukhin,[a,c] Mikhail B. Berezin,[a] and Elena V. Antina[a]

[a]*G.A. Krestov Institute of Solution Chemistry of the Russian Academy of Sciences, 153045 Ivanovo, Russia*
[b]*Ivanovo State University of Chemistry and Technology, 153000 Ivanovo, Russia*
[c]*Ivanovo State University, 153025 Ivanovo, Russia*
[@]*Corresponding author E-mail: artsherudillo@gmail.com*

*Bromine-substituted BODIPY photosensitizers exhibiting intense absorption and efficient singlet oxygen generation in the visible spectral region are promising candidates for applications in antimicrobial photodynamic therapy. This work presents a methodology for the synthesis of a novel asymmetrically brominated BODIPY photosensitizer (BODIPY **2**) and the results of a comparative study of its spectral characteristics and photodynamic antimicrobial activity against S. aureus and E. coli bacterial strains. It was found that the asymmetric substitution of the pyrrole rings with bromine atoms does not significantly affect the photophysical and photochemical characteristics of the BODIPY photosensitizer compared to its symmetrically substituted analogues. Experimental data revealed that BODIPY **2** exhibited superior photodynamic activity against S. aureus, reducing their viability to 0.04 % even at a minimal photosensitizer concentration of ~1 μM.*

Keywords: Unsymmetrically substituted BODIPYs, photosensitizers, chromophoric characteristics, fluorescence, antimicrobial activity.

Новый несимметрично замещенный дибром-BODIPY фотосенсибилизатор: синтез, фотофизические/фотохимические характеристики и антимикробная активность

Л. А. Антина,[a] Д. А. Федорова,[a,b] А. С. Шерудилло,[a@] О. В. Милошевская,[a,b] А. Н. Сивухин,[a,c] М. Б. Березин,[a] Е. В. Антина[a]

[a]*Институт химии растворов им. Г.А. Крестова Российской академии наук, 153045 Иваново, Россия*
[b]*Ивановский государственный химико-технологический университет, 153000 Иваново, Россия*
[c]*Ивановский государственный университет, 153025 Иваново, Россия*
[@]*E-mail: artsherudillo@gmail.com*

*Бромзамещенные BODIPY фотосенсибилизаторы, демонстрирующие интенсивное поглощение и эффективное образование синглетного кислорода в видимой области спектра, являются перспективными кандидатами для применения в антимикробной фотодинамической терапии. В данной работе представлена методология синтеза нового несимметрично бромированного фотосенсибилизатора BODIPY (BODIPY **2**) и результаты сравнительного исследования его спектральных характеристик и фотодинамической антимикробной активности в отношении бактериальных штаммов S. aureus и E. coli. Было установлено, что несимметричное замещение пиррольных колец атомами брома не оказывает существенного влияния на фотофизические и фотохимические характеристики фотосенсибилизатора BODIPY по сравнению с его симмет-*

рично замещенными аналогами. Экспериментальные данные показали, что BODIPY 2 обладает превосходной фотодинамической активностью в отношении S. aureus, снижая их жизнеспособность до 0,04 % даже при минимальной концентрации фотосенсибилизатора ~1 мкМ.

Ключевые слова: Несимметрично замещенные BODIPY, фотосенсибилизаторы, хромофорные характеристики, флуоресцентция, антимикробная активность.

Introduction

Bacterial infections pose one of the most significant healthcare challenges. Until recently, the use of antibiotics allowed this problem to be successfully managed, but their overuse has led to the emergence and rapid proliferation of bacteria with multidrug resistance.[1,2] The development of new antibiotics does not provide a long-term successful solution to this problem. Antibacterial photodynamic therapy (PDT) is proposed as one of the promising alternative methods for treating bacterial infections.[3–5] The antibacterial PDT method is based on irradiation with certain wavelength light of photosensitizers (PSs) which are capable of generating reactive oxygen species (ROS) that induce the death of pathogenic microorganisms without promoting the development of resistance. Compared with traditional antibiotic therapy, the antibacterial PDT method can additionally provide higher selectivity, less invasiveness, minimal side effects, and the possibility of repeated prophylactic therapy. The choice of a suitable photosensitizer (PS) is of critical importance for the effective treatment of infectious diseases, making the development of highly efficient photodynamic agents a most urgent task.

BODIPY-based photosensitizers have already proven their effectiveness in the photodynamic inactivation of bacterial infections and continue to attract unabated attention due to their excellent spectral properties, photostability, biocompatibility and good membrane permeability, ease of synthesis and the possibility of structural modification.[6–11] The classical strategy for achieving efficient BODIPY photosensitizers is based on the “heavy atom effect”. The incorporation of heavy atoms (*e.g.*, Pd, Pt, Br, I) into the BODIPY structure promotes intersystem crossing to the triplet state, thereby facilitating the generation of reactive oxygen species and enabling photodynamic therapy.[12–19] The incorporation of bromine atoms into the BODIPY molecular structure is considered the most optimal strategy, since it avoids significant synthetic expenses and a critical increase in the dark toxicity of the photosensitizer.[20-23] Furthermore, for bromo-substituted BODIPYs, a successful combination of optimal fluorescence, $^1O_2$ generation and photostability can be achieved.[20,24-26]

As our previous studies have shown, not only the nature and number of heavy atoms introduced into the BODIPY structure, but also their attachment positions, have a significant impact on the entire set of practically relevant characteristics of the PS: spectral (chromophoric, fluorescent) properties, singlet oxygen generation efficiency, membrane permeability, cellular localization, and PDT efficiency.[24,25] In this regard, we obtained an asymmetrically substituted tetramethyl-BODIPYs with unsubstituted β,β'-positions (BODIPY **1**) and its β,β'-dibromo-substituted derivative – β,β'-diBr-BODIPY (BODIPY **2**) (Figure 1). A primary goal of this research was to investigate the effect of asymmetric substitution in the pyrrole rings of BODIPY molecules on their spectral properties (Figure 1). The main objectives included the synthesis of a new PS based on asymmetrically substituted BODIPY **2** and a comparative analysis of its spectral characteristics with those of the non-brominated precursor BODIPY **1** (Figure 1). Additionally, the study aimed to assess its photodynamic antibacterial activity against *S. aureus* and *E. coli* bacterial strains.

Experimental

General

All organic solvents used were of spectrophotometric grade (for analysis, Panreac, Barcelona) and were used without further purification.

The ^1H and ^{13}C spectra were obtained using a Bruker Avance - III 500 MHz spectrometer to determine the BODIPYs

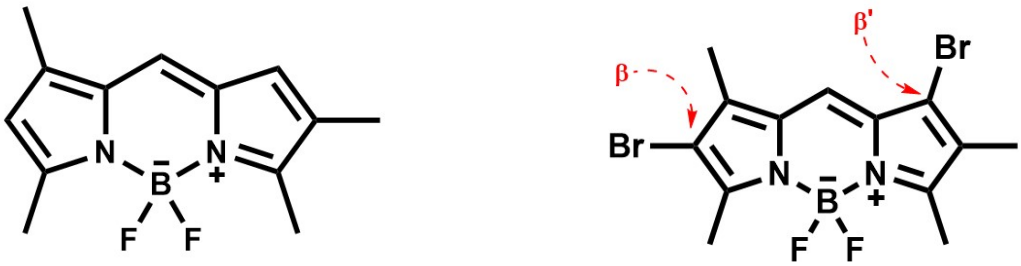

BODIPY 1 **BODIPY 2**

Figure 1. Objects of the study BODIPYs: 3,4',5,5'-tetramethyl-2,2'-dipyrrolylmethene difluoroborate (BODIPY 1) and 3',4-dibromo-3,4',5,5'-tetramethyl-2,2'-dipyrrolylmethene difluoroborate (BODIPY 2) (The red arrows indicate the positions of attachment of bromine atoms).

structure. The operating frequency for the cores was 500.17 MHz. Sample preparation was done in standard NMR ampoules (OD = 5 mm) with deuterated chloroform as a solvent and a small amount (0.03 % v/v) of TMS as an internal standard. The temperature was maintained at 25 °C using temperature control units (Bruker BVT-2000) and cooling units (Bruker BCU 05). All NMR spectra were recorded using the pulse programs included in the software package of the TopSpin 3.6.1 spectrometer. The ^{1}H NMR spectra were recorded in the spectral range of 12.4 ppm, with 32 scans, a relaxation delay (d1) of 3 seconds, and 32768 data points. Mass spectra were recorded on a Shimadzu AXIMA Confidence MALDI TOF mass spectrometer in positive ion reflection mode. Electronic absorption spectra were recorded on a CM 2203 spectrometer (SOLAR, Belarus). The fluorescence spectra of dye solutions were recorded on RF-6000 spectrofluorimeter (Shimadzu, Japan). The time-resolved fluorescence measurements were performed using a high-performance FluoTime 300 spectrometer (PicoQuant) with a LDH-P-C-500 (PicoQuant) as excitation sources. The measurements were carried out for dilute dye solutions: optical density (A) at the maximum of the intense emission band ≤ 0.1. The instrument response function (IRF) of the system was measured using the stray light signal of the dilute colloidal silica suspension (LUDOX®). The fluorescence lifetimes were obtained by reconvolution of the decay curves using the EasyTau 2 software package (PicoQuant, Germany).

Photophysical and photochemical study

The fluorescence quantum yield (Φ_{fluo}) of the dyes in organic solvents was determined on RF-6000 (Shimadzu, Japan) using an integration sphere with excitation at 500 nm. The radiative (k_{rad}), and non-radiative (k_{nrad}) process constants were determined with the following equations (1) and (2):

$$k_{rad} = \frac{\Phi_{fluo}}{\tau_{fluo}}\left(s^{-1}\right), \quad (1)$$

$$k_{nrad} = \frac{\left(1-\Phi_{fluo}\right)}{\tau_{fluo}}\left(s^{-1}\right), \quad (2)$$

where Φ_{fluo} – is fluorescence quantum yield; τ_{fluo} – fluorescence lifetime (ns).

The singlet oxygen quantum yield (Φ_Δ) was determined from the characteristics of $^1O_2$ luminescence. The data were recorded with a spectrometer FluoTime 300 (PicoQuant), equipped NIR detector, and a laser LDH-P-C-500 (PicoQuant) served as the excitation source. Rose bengal (BR) and tetraphenylporphine (TPP) solutions with known values of Φ_Δ in the corresponding solvents were used as standards. The control of dyes stability by absorption spectra before and after the experiment were carried out and the destruction of complexes under laser exposure was not observed. Measurements of the dye and the standard were carried out in the same solvent under the same conditions. The Φ_Δ values were calculated using Equation 3:

$$\Phi_\Delta = \Phi_{\Delta st} \cdot \left(\frac{\alpha_{st}}{\alpha_{BODIPY}}\right) \cdot \left(\frac{Se_{BODIPY}}{Se_{st}}\right), \quad (3)$$

where $\Phi_{\Delta st}$ is the quantum yield of $^1O_2$ generation for the used standard; factor $\alpha = 1\text{-}10^{-A\text{bs}}$, corrects the different amounts of photons absorbed by the sample (α_{BODIPY}) and reference (α_{st}); factor *Se* is the intensity of the $^1O_2$ phosphorescence signal of the sample (Se_{BODIPY}) and the reference (Se_{st}) at 1275 nm. The $^1O_2$ quantum yields were averaged from several concentrations.

Synthetic procedures of BODIPYs

3,5,4′,5′-Tetramethyl-2,2′-dipyrrolylmethene hydrobromide, $C_{13}H_{17}N_2$; M = 281.20 g/mol was prepared from 2,4-dimethylpyrrole and 2,3-dimethyl-5-formylpyrrole (Scheme 1). 0.75 g (7.88 mmol) of 2,4-dimethylpyrrole and 0.97 g (7.88 mmol) of 2,3-dimethyl-5-formylpyrrole were dissolved in 4 mL of methanol, and 1.5 mL of concentrated HBr was added. The mixture was stirred for 2 hours at room temperature. Then, 25 mL of ether was added dropwise to the reaction mixture. The mixture was stirred for 5 minutes, and the solution was decanted from the precipitate. The precipitate was boiled with 50 mL of benzene, filtered, and dried under vacuum. Yield 1.99 g (7.07 mmol, 90%). Electronic absorption spectrum (CH_2Cl_2) λ_{max} nm: 477, 356. ^{1}H NMR ($CDCl_3$) δ_H ppm: 13.30 (bs, 1H, NH); 13.09 (bs, 1H, NH); 6.97 (s, 1H, CH); 6.85 (s, 1H, CH); 6.14 (s, 1H, *ms*-H); 2.67 (s, 3H, -CH_3); 2.65 (s, 3H, -CH_3); 2.31 (s, 3H, -CH_3); 2.05 (s, 3H, -CH_3). ^{13}C NMR ($CDCl_3$) δ_C ppm: 156.49; 155.96; 146.92; 134.23; 127.90; 127.24; 127.08; 123.57; 118.26; 15.13; 13.50; 12.71; 11.24.

*3,4′,5,5′-Tetramethyl-2,2′-dipyrromethene difluoroborate (BODIPY **1**)*, $BF_2C_{13}H_{15}N_2$; M = 248.08 g/mol, was synthesized *via* complexation reaction (Scheme 2). 0.250 g (0.889 mmol) of 3,5,4',5'-tetramethyl-2,2'-dipyrromethene hydrobromide was dissolved in 40 mL of anhydrous dichloromethane (DCM), and 0.93 mL (5.33 mmol) of N,N-diisipropylethylamine (DIPEA) was added. The solution was stirred for 5 min. Then, 0.89 mL (7.12 mmol) of $BF_3{\cdot}Et_2O$ was added dropwise, and the mixture was stirred for 3 h at room temperature. The red-orange solution was evaporated, adsorbed onto 3 mL of silica gel, and chromatographed on silica gel, eluting with a petroleum ether–dichloromethane mixture (1/1). The solvent was partially distilled off, the residue was cooled, and the product was filtered off. Yield: 0.179 g (0.721 mmol, 81%) MALDI TOF *m/z*: found $[M]^+$= 248.24, calculated $C_{13}H_{15}BF_2N_2$; $[M]^+$=248.08. ^{1}H NMR ($CDCl_3$) δ_H ppm: 6.97 (s, 1H, C-H); 6.71 (s, 1H, C-H); 6.05 (s, 1H, *ms*-H); 2.56 (s, 3H, -CH_3); 2.53 (s, 3H, -CH_3); 2.24 (s, 3H, -CH_3); 2.06 (s, 3H, -CH_3). ^{13}C NMR ($CDCl_3$) δ_C ppm: 157.69; 156.56; 142.08; 134.47; 133.24; 128.56; 128.34; 122.88; 119.57; 15.27; 13.26; 11.81; 11.69.

*3′,4-Dibromo-3,4′,5,5′-tetramethyl-2,2′-dipyrromethene difluoroborate (BODIPY **2**)*, $BF_2C_{13}H_{13}Br_2N_2$; M= 405.87 g/mol was synthesized according to Scheme 3. At room temperature, a solution of 0.740 g (4.16 mmol) of N-bromosuccinimide (NBS) in 20 mL of anhydrous tetrahydrofurane (THF) was added dropwise slowly (over ≈ 45 min) to a solution of 0.172 g (0.693 mmol) of BF_2-3,5,4',5'-tetramethyl-2,2'-dipyrromethene in 10 mL of anhydrous THF. The mixture was stirred at room temperature for an additional 3 h (monitored by TLC). The precipitated 3′,4-dibromo-3,4′,5,5′-tetramethyl-2,2′-dipyrromethene difluoroborate was filtered off and washed with CH_2Cl_2**.** The filtrate was washed with a saturated aqueous solution of sodium thiosulfate (2 × 20 mL), the organic layer was separated and dried over Na_2SO_4. The drying agent was filtered off, and the solvent was removed under vacuum. The residue was dissolved in methylene chloride, adsorbed onto 2 mL of silica gel, and chromatographed on silica gel with a petroleum ether-CH_2Cl_2 mixture (1:1 v/v). The solvent was partially evaporated, and the mixture was cooled. The precipitated product was filtered off and dried under vacuum. Yield: 0.154 g (0.379 mmol, 55%). Electronic absorption spectrum (CH_2Cl_2) λ_{max} nm: 534, 378**.** MALDI TOF *m/z*: found: $[M+H]^+$ = 406.52, calculated: $BF_2C_{13}H_{13}Br_2N_2$; $[M]^+$ = 405.87. ^{1}H NMR ($CDCl_3$) δ_H ppm: 7.12 (s, 1H, *ms*-H); 2.57 (s, 3H, CH_3); 2.56 (s, 3H, CH_3); 2.26 (s, 3H, CH_3); 2.05 (s, 3H, CH_3). ^{13}C NMR ($CDCl_3$) δ_C ppm: 156.59; 155.59; 139.97; 132.79; 132.08; 128.38; 121.39; 120.88; 110.19; 14.15; 13.90; 11.71; 10.87.

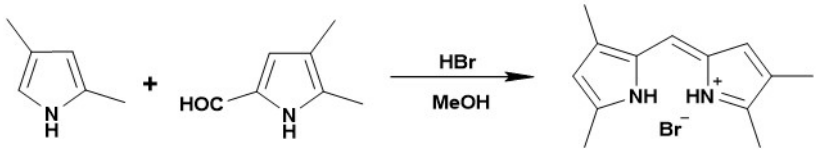

Scheme 1. The synthesis of 3,5,4',5'-tetramethyl-2,2'-dipyrromethene hydrobromide.

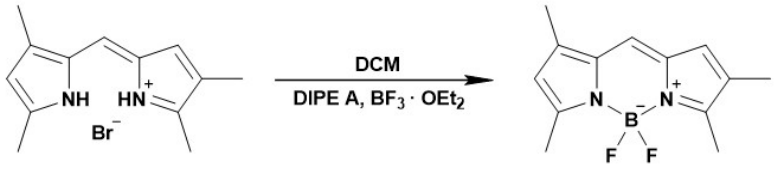

Scheme 2. The synthesis of 3,4',5,5'-tetramethyl-2,2'-dipyrromethene difluoroborate (BODIPY **1**).

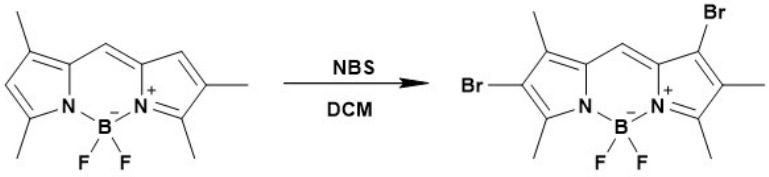

Scheme 3. The synthesis of 3′,4-dibromo-3,4',5,5'-tetramethyl-2,2'-dipyrromethene difluoroborate (BODIPY **2**).

Antimicrobial activity

To determine the antimicrobial activity of BODIPY **2**, strains of Gram-positive (*S. aureus*) and Gram-negative (*E. coli*) bacteria were used. A pure culture was first isolated from wild-type strains and cultured on slant agar at a temperature of 37 °C. The photosensitizer under study was introduced into a suspension of microorganisms (in physiological saline in test tubes), followed by inoculation of Petri dishes containing solid agar using the lawn method. For cultivating *S. aureus*, salt agar (Staphylococcus Agar, TU 9398-109-78095326-2010) was used; for *E. coli*, Nutrient Agar was used. Irradiation of the experimental suspensions was carried out using a green LED assembly with an intensity of 3000 lux (0.79 J/cm²) on the surface of the test tube. After all procedures, the cultures were placed in a thermostat at 37°C for 24 hours. Colonies were counted using a Micromed MC-1 binocular microscope at 40× magnification. To identify and assess the physiological state of the bacterial cells, colonies were stained by the Gram method and, routinely, with an aqueous-alcoholic gentian violet solution. Microscopic analysis was then performed using a Micromed R-1 LED microscope at ×1600 magnification with an oil-immersion objective.

The viability (%) of bacteria was estimated using the Equation 4:

$$Viability = \frac{CFU_{survived}}{CFU_{control}} \cdot 100\%, \quad (4)$$

where $CFU_{survived}$ – the number of colony-forming units counted in the sample that received the treatment, $CFU_{control}$ – the number of colony- forming units counted in the control sample, which is treated identically except for the absence of the active treatment.

The IC_{50} (μM) value was determined from the concentration-viability curve. Viability data were plotted as a function of photosensitizer concentration, and the concentration corresponding to 50% viability was interpolated from the curve: Viability = *f*(C).

Results and Discussion

*Spectral characteristics of BODIPY dyes **1**, **2***

The synthesized dyes **1** and **2** have the absorption spectra typical for monochromophoric alkyl- and alkylbromo substituted BODIPY dyes (Figure 2a,b).[20] Like the previously studied symmetrically substituted analogs,[23–26] BODIPYs **1** and **2** exhibit strong absorption in the visible region of the spectrum with high extinction coefficients (the lgε values range from 4.84 to 5.00) (Table 1, Figure 2a,b). In the solvents studied, the maximum of the intense absorption band of asymmetric tetramethyl-BODIPY **1** is recorded in the range from 517 to 525 nm, and its brominated derivative BODIPY **2** – in the range from 529 to 540 nm (Table 1). Bromination of the β,β'-positions of pyrroles leads to a noticeable – up to 16 nm – bathochromic shift of the BODIPY **2** absorption band in comparison with BODIPY **1** under similar environmental conditions (Table 1). Comparison with the chromophore characteristics of symmetrically substituted brominated BODIPY analogs showed that the violation of the symmetry of the pyrrole ring position substitution with bromine atoms does not have any noticeable effect on the position of the intense absorption band maximum of the dye, the range of which is 529–540, 528–539 and 531–538 nm in the spectra of β,β'-diBr-BODIPY, β,β-diBr-BODIPY and β',β'-diBr-BODIPY dyes, respectively[25] (Table 1, Table S1). The solvatochromic effect for both BODIPY **1** and its halogenated derivative BODIPY **2** is small and consists of a blue shift of the intense absorption band maximum to 8 nm and 11 nm, respectively (Table 1).

The fluorescence spectra of BODIPY **1** and **2** have one high-intensity band and are mirror images of the absorption spectra (Figure 2c,d). The fluorescence bands maxima of asymmetric methylated BODIPY **1** are in the

range from 525 to 531 nm, and of its brominated derivative BODIPY **2** are in the range from 539 to 547 nm (Table 1), i.e. shifted to the long-wavelength region of the spectrum from 13 to 16 nm compared to the unbrominated precursor **1** (under the same environmental conditions) (Table 1). The range of the emission band maximum of asymmetrically brominated BODIPY **2** is comparable to the values range of symmetrically brominated analogs: β,β-Br-BODIPY (544–549 nm) and β',β'-Br-BODIPY (544–552 nm) (Table S1).[25] Bromination of the dye does not have any significant effect on the Stokes shift values, which for BODIPY **1** and BODIPY **2** are in the ranges of 146–401 and 173–351 cm^{-1}, respectively (Table 1).

As a result of the "heavy atom effect" and the consequent increase in the efficiency of intersystem crossing: the k_{nrad} values for dye **1** are up to seven times higher compared to dye **2** (Table S1); the fluorescence quantum yield of brominated BODIPY **2** is expectedly lower compared to the unbrominated precursor BODIPY **1** (the Φ_{fluo} values range from 15 to 32 % and from 66 to 77 % for dyes **2** and **1** respectively); the fluorescence lifetime of BODIPY **2** is reduced by a factor of up to five relative to the non-brominated precursor (the fluorescence decays are well described by a biexponential model) (Table 1, Figure S9).

To quantitatively describe the solvatochromism of BODIPY **1** and BODIPY **2**, we performed simple linear and multiple regression (MLR) analysis of the photophysical characteristics of the dyes from a standard set of solvent parameters (polarity, basicity and acidity, including the Catalan and Kamlet-Taft scales, as well as density, dipole moment and refractive index) using the SolvatoChrom web tool (https://solvatochrome.isc-ras.ru/). The regression analysis protocols BODIPY **1** and BODIPY **2** are provided in the *Supporting Information*. When using simple linear analysis, no reasonable correlations were obtained. The results of the multiple linear regression analysis also revealed a low correlation for the fluorescence quantum yield and fluorescence lifetime of both dyes in all cases. The maximum correlation coefficient, observed for both BODIPY **1** and BODIPY **2** (with $R^2 = 0.96$ and $R^2 = 0.95$, respectively) was obtained for the MLR of the absorption band maximum position using the four-parameter Catalan scale. For both BODIPY **1** and BODIPY **2**, the greatest contribution is made by the polarizability parameter SP, indicating that the variation in the absorption band position of the dyes as a function of the solvent is primarily governed by differences in the electronic polarizability of the solvents, rather than by their acid–base properties or dipole moments.

The quantum yield of singlet oxygen generation of non-halogenated BODIPY **1** does not exceed 8 % (Table 1). The efficiency of singlet oxygen generation by asymmetrically brominated BODIPY **2** reaches 45–83 % depending on the nature of the solvent (Table 1, Figure S10). Consequently, BODIPY **2** exhibits efficient visible-light-induced singlet oxygen generation, with an efficiency comparable to its symmetrically brominated β,β-Br-BODIPY and β',β'-Br-BODIPY analogues (Table S1).[25] In connection with this, an investigation of its phototoxicity against Gram-positive (*S. aureus*) and Gram-negative (*E. coli*) pathogenic bacteria was carried out.

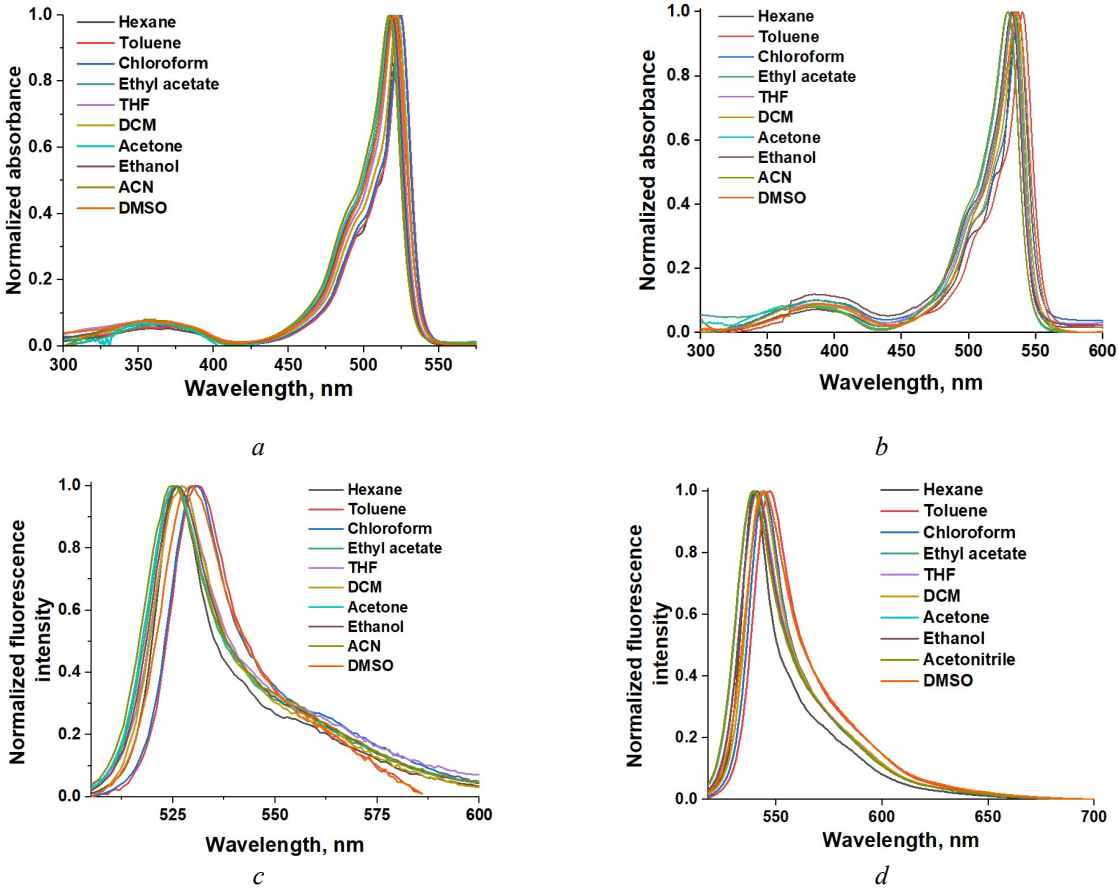

Figure 2. Normalized absorption spectra of BODIPY **1** (a) and BODIPY **2** (b); normalized fluorescence spectra of BODIPY **1** (c) and BODIPY **2** (d).

Table 1. Spectral characteristics of BODIPYs **1** and **2** in organic solvents (T = 25°C).

Solvent	λ^{abs}, nm	lgε	λ^{fluo}, nm	$\Delta\upsilon_{ss}$, cm^{-1}	Φ_{fluo}	τ_{fluo}, ns	$k_{rad} \cdot 10^{-8}$, s^{-1}	$k_{nrad} \cdot 10^{-8}$, s^{-1}	Φ_{Δ} ($^1O_2$)
BODIPY **1**									
Hexane	522	5.00	526	146	0.66	6.17	1.07	0.55	-
Toluene	525	4.93	531	215	0.72	5.25	1.37	0.53	0.05
Chloroform	524	4.94	530	216	0.74	5.89	1.26	0.44	0.02
THF	520	4.91	527	255	0.69	5.71	1.21	0.54	0.05
Ethyl acetate	518	4.87	529	401	0.77	6.02	1.28	0.38	-
CH_2Cl_2	522	4.91	529	253	0.73	6.00	1.22	0.45	-
Acetone	518	4.90	526	294	0.76	6.22	1.22	0.39	-
Ethanol	519	4.86	526	256	0.70	6.24	1.12	0.48	0.08
Acetonitrile	517	4.85	525	295	0.68	6.29	1.08	0.51	0.07
DMSO	520	4.86	530	363	0.69	5.46	1.26	0.57	-
BODIPY **2**									
Hexane	535	5.01	540	173	0.32	2.23	0.32	2.23	-
Toluene	540	4.93	547	237	0.31	1.49	0.31	1.49	0.71
Chloroform	537	4.91	544	240	0.29	2.09	0.29	2.09	0.45
THF	533	4.92	541	277	0.26	1.58	0.26	1.58	0.62
Ethyl acetate	534	4.91	540	208	0.26	1.59	0.26	1.59	-
CH_2Cl_2	535	5.00	543	275	0.25	1.82	0.25	1.82	-
Acetone	529	4.90	539	351	0.19	1.33	0.19	1.33	-
Ethanol	532	4.69	541	313	0.22	1.99	0.22	1.99	0.62
Acetonitrile	529	4.84	539	351	0.15	1.30	0.15	1.30	0.83
DMSO	536	4.87	544	274	0.18	1.24	0.18	1.24	-

Note: absorption maxima (λ^{abs}, nm), molar absorption coefficients (lgε), emission maxima (λ^{fluo}, nm), Stokes shift ($\Delta\upsilon_{ss}$, cm^{-1}), fluorescence quantum yield (Φ_{fluo}), fluorescence lifetime (τ_{fluo}, ns), the radiative and non-radiative rate constants (k_{rad} and k_{nrad}, s^{-1}), singlet oxygen quantum yield (Φ_{Δ} ($^1O_2$)).

Antimicrobial Activity of BODIPY 2

The photodynamic activity of BODIPY **2** was evaluated against Gram-positive (*Staphylococcus aureus*) and Gram-negative (*Escherichia coli*) bacteria. Irradiation was performed using a green LED source (0.79 J/cm²). Experiments (without irradiation, Figure 3a,b, red lines) demonstrated that BODIPY **2** exhibited no dark toxicity within the concentration range studied (1–30 μM) for both bacterial strains tested. It is important to note that in dark experiments, an increase in CFU counts was observed in the presence of DMSO (the solvent for BODIPY **2**) for both strains (Figure 3a,b, red lines), which is consistent with previously published data[27] and is attributed to the dissociating effect of DMSO on bacterial aggregates rather than to actual biomass growth.

Against *S. aureus*, BODIPY **2** showed pronounced photoinduced activity in a dose-dependent manner. At a concentration of just 1 μM, a 99.96% reduction in CFU was observed compared to the control (survival rate 0.037%) (Figure 3a, black line). The calculated half-maximal inhibitory concentration (IC_{50}) was 0.14 μM. In contrast to the Gram-positive culture, BODIPY **2** did not exert a significant photodynamic effect on *E. coli* within the concentration range studied (Figure 3b, black line). Even at the maximum concentration (30 μM), no decrease in the survival rate of Gram-negative bacteria was observed (Figure 3b).

The differences in viability between the two bacterial types following treatment with the photosensitizer BODIPY **2** are attributed to the structural features of the cell wall. In Gram-negative bacteria, the presence of an outer membrane containing lipopolysaccharides creates an effective barrier against the hydrophobic BODIPY molecules.

Conversely, the peptidoglycan layer of Gram-positive *S. aureus* does not impede the penetration of the photosensitizer to the cytoplasmic membrane, thereby ensuring the high efficacy of the photodynamic effect.

Conclusions

For the first time, asymmetrically substituted tetramethyl-BODIPY **1** and its dibromo-substituted derivative BODIPY **2** have been synthesized. It was found that BODIPY **2** photosensitizer, exhibits intense absorption and fluorescence in the visible spectral region, and efficiently generates singlet oxygen. A comparative analysis of the BODIPY **2** optical properties showed that the asymmetry of substitution of the BODIPY molecule pyrrole rings does not cause significant changes in its spectral characteristics compared to symmetrically brominated analogues. Upon exposure to visible light, BODIPY **2** exhibits a significant

inhibitory effect on *S. aureus*, reducing survival to as low as 0.04 % even at the minimum photosensitizer concentration. The BODIPY **2** photosensitizer does not exhibit a noticeable inhibitory effect on *E. coli*. In subsequent stages of the study, it is planned to obtain chitosan/BODIPY **2** polymer composites and investigate their antimicrobial activity against a range of pathogenic microorganisms.

Acknowledgments. This work was supported by Russian Science Foundation together with the Government of Ivanovo Region, Grant No. 25-23-20149 (https://rscf.ru/project/25-23-20149/). This research was carried out with the help of the Centre for Joint Use of Scientific Equipment «The Upper Volga Region Centre of Physico-Chemical Research» and the Center for Shared Use of Scientific Equipment of Ivanovo State University of Chemistry and Technology.

Author Contribution. L.A. Antina: conceptualization; writing – review and editing; supervision; funding acquisition. D.A. Fedorova: investigation; writing – original draft. A.S. Sherudillo: investigation; writing – original draft; visualization; formal analysis. O.V. Miloshevskaya: investigation; visualization; formal analysis. A.N. Sivukhin: methodology; investigation; validation; resources; writing – original draft. M.B. Berezin: writing – review and editing; supervision; resources; methodology. E.V. Antina: conceptualization; writing – review and editing; supervision; project administration.

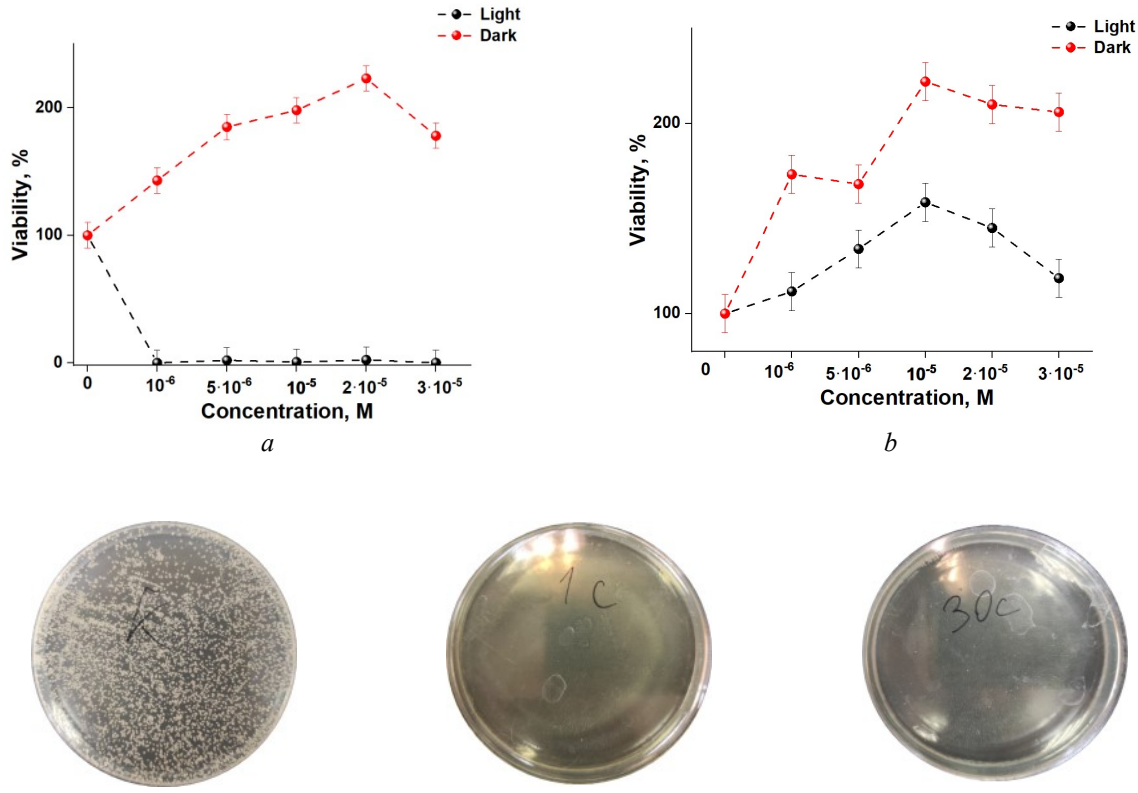

Figure 3. Antibacterial efficiencies of BODIPY **2** against *S. aureus* (a) and *E. coli* (b) with (red dotted line) and without (black dotted line) green light irradiation (0.76 J/cm^2); images of Petri dishes (c) containing *S. aureus* after irradiation with different concentrations of BODIPY **2.** Data are presented as mean values from three independent experiments.

References

1. Salam Md.T., Bari K.F., Rahman Md.M., et al. *J. Angiotherapy* **2024**, *8*(5), 9560. https://doi.org/10.25163/angiotherapy.859560.
2 Kim J., Ahn J. *Food Sci. Biotechnol.* **2022**, *31*, 1481; https://doi.org/10.1007/s10068-022-01157-1.
3 Ghorbani J., Rahban D., Aghamiri S., Teymouri A., Bahador A. *Laser Ther.* **2018**, *27*, 293; https://doi.org/10.5978/islsm.27_18-RA-01.
4 He C., Feng P., Hao M., Tang Y., Wu X., Cui W., Ma J., Ke C. *Adv Funct. Mater.* **2024**, *34*, 8631; https://doi.org/10.1002/adfm.202402588.
5 Maisch T., Szeimies R.-M., Jori G., Abels C. *Photochem. Photobiol. Sci.* **2004**, *3*, 907; https://doi.org/10.1039/B407622B.
6 Awuah S.G., You Y. *RSC Adv.* **2012**, *2*, 11169; https://doi.org/10.1039/C2RA21404K.
7 Guan Y., Yu B., Ding J., Sun T., Xie Z. *Chin. Chem. Lett.* **2025**, *36*, 110645; https://doi.org/10.1016/j.cclet.2024.110645.
8 Orlandi V.T., Martegani E., Bolognese F., Caruso E. *Photochem. Photobiol. Sci.* **2022**, *21*, 1233; https://doi.org/10.1007/s43630-022-00212-4.
9 Liang X., Xia L., Zhu Y., Zhang C., Gong F., Zhang W. *Biomater. Sci.* **2022**, *10*, 4235; https://doi.org/10.1039/D2BM00780K.

10 Liu B.-K., Zheng J., Wang H., Niu L.-Y., Yang Q.-Z. *Mater. Chem. Front.* **2023**, *7*, 5879; https://doi.org/10.1039/D3QM00753G.
11 Kamkaew A., Lim S.H., Lee H.B., Kiew L.V., Chung L.Y., Burgess K. *Chem. Soc. Rev.* **2013**, *42*, 77; https://doi.org/10.1039/c2cs35216h.
12 Kim B., Sui B., Yue X., Tang S., Tichy M.G., Belfield K.D. *Eur. J. Org. Chem.* **2017**, *2017*, 25; https://doi.org/10.1002/ejoc.201601054.
13 Filatov M.A. *Org. Biomol. Chem.* **2019**, *18*, 10; https://doi.org/10.1039/C9OB02170A.
14 Kim C., Kim H., Jo J., Kim S., Bongo A.M., Kim H.-J., Yang J. *ACS Appl. Bio Mater.* **2024**, *7*, 8294; https://doi.org/10.1021/acsabm.4c01108.
15 Rey Y.P., Abradelo D.G., Santschi N., Strassert C.A., Gilmour R. *Eur. J. Org. Chem.* **2017**, *2017*, 2170; https://doi.org/ 10.1002/ejoc.201601372.
16 Wang J., Gong Q., Wang L., Hao E., Jiao L. *J. Porphyrins Phthalocyanines* **2020**, *24*, 603; https://doi.org/10.1142/S1088424619300234.
17 Zou J., Yin Z., Ding K., Tang Q., Li J., Si W., Shao J., Zhang Q., Huang W., Dong X. *ACS Appl. Mater. Interfaces* **2017**, *9*, 32475; https://doi.org/10.1021/acsami.7b07569.
18 Turksoy A., Yildiz D., Akkaya E.U. *Coord. Chem. Rev.* **2019**, *379*, 47; https://doi.org/10.1016/j.ccr.2017.09.029.
19 Kerner A.A., Borisovskaya E.P., Krestova A.N., Ksenofontov A.A., Molchanov E.E., Ksenofontova K.V. *Ross. Khim. Zh. (Russian Chemistry Journal)* **2024**, *68*(2), 121-124. https://rcj-isuct.ru/article/view/5902
20 Bumagina N.A., Antina E.V., Ksenofontov A.A., Antina L.A., Kalyagin A.A., Berezin M.B. *Coord. Chem. Rev.* **2022**, *469*, 214684; https://doi.org/10.1016/j.ccr.2022.214684.
21 Cheng H.-B., Cao X., Zhang S., Zhang K., Cheng Y., Wang J., Zhao J., Zhou L., Liang X.-J., Yoon J. *Adv. Mater.* **2023**, *35*, e2207546; https://doi.org/10.1002/adma.202207546.
22 Mao Z., Kim J.H., Lee J., Xiong H., Zhang F., Kim J.S. *Coord. Chem. Rev.* **2023**, *476*, 214908; https://doi.org/10.1016/j.ccr. 2022.214908.
23 Hu W., Zhang R., Zhang X.-F., Liu J., Luo L. *Spectrochim. Acta A Mol. Biomol. Spectrosc.* **2022**, *272*, 120965; https://doi.org/10.1016/j.saa.2022.120965.
24 Dogadaeva S.A., Antina L.A., Ksenofontov A.A., Kalyagin A.A., Khodov I.A., Berezin M.B., Antina E.V., Pavelyev R.S., Frantsuzova L.V., Lodochnikova O.A., Islamov D.R. *J. Mol. Liq.* **2023**, *382*, 121892; https://doi.org/10.1016/j.molliq. 2023.121892.
25 Dogadaeva S.A., Kalyagin A.A., Ksenofontov A.A., Antina L.A., Berezin M.B., Antina E.V., Semeikin A.S. *Macroheterocycles* **2024**, *17*, 322; https://doi.org/10.6060/mhc245846d.
26 Nuraneeva E.N., Guseva G.B., Antina E.V., V'yugin A.I. *J. Photochem. Photobiol. A: Chem.* **2022**, *426*, 113789; https://doi.org/10.1016/j.jphotochem.2022.113789.
27 Sivukhin A.N., Sherudillo A.S. *International Journal of Applied and Basic Research [Международный журнал прикладных и фундаментальных исследований]* **2025**, (12), 5-8; https://doi.org/10.17513/mjpfi.13773.

Received 03.03.2026
Accepted 04.04.2026